MWCL-21-0192

Nonlinear Analysis of a High-Power Oscillator Inductively Coupled to an External Resonator

Víctor Ardila, Franco Ramírez, *Senior Member*, IEEE, and Almudena Suárez, *Fellow, IEEE*

***Abstract*— This contribution presents a detailed nonlinear analysis of a high-power oscillator that is inductively coupled to an external resonator for power transfer applications. The analytical formulation of a cubic nonlinearity oscillator enables the derivation of the maximum transferred power and the value of the coupling factor at which the oscillation is extinguished. Then, a simple procedure to obtain a Class-E oscillator from an initial high efficiency oscillator is presented. The solution curves versus the coupling factor and the elements of the external resonator are easily obtained from the extraction of a bi-variate nonlinear admittance function accounting for the oscillator circuit, which is combined with the passive admittance of the coupled resonator. Very good correspondence has been obtained between simulation and measured results.**

***Index Terms*— Oscillator, inductive coupling, bifurcation.**

I. Introduction

SEVERAL recent works propose the use of a high-power oscillator as the excitation source of near-field inductive power transfer systems [1]-[4], which avoids the need of both an independent generator and an amplifier. The transferred power and efficiency depend on the distance between the coils [5], which will affect the robustness of the coupled system. Most previous works [1]-[4] are devoted to analyze/optimize the efficiency of the transfer process, and, to the best of our knowledge, no detailed investigation has been carried out yet of the variations in the oscillator solution (maximum power transfer, oscillation hysteresis, multivalued operation, etc.) versus the coupling factor. Because in the power transfer application, the output resistive load is located in the external resonator, one can expect the behavior to be different from that of the voltage-controlled oscillator in [6],[7], which had its own output load and was coupled to a high-quality factor resonator.

To investigate the behavior, we will initially consider a simple cubic-nonlinearity oscillator. We will analyze the variation of the oscillation frequency and power transfer versus the coupling factor. Using the derived formulation, we will determine the maximum transferred power and obtain the coupling conditions for the oscillation extinction. Then, a practical transistor-based oscillator will be considered. With this aim, we will use a simple feedback procedure to transform a Class-E amplifier into a high power and high efficiency oscillator. The solution curves (in terms of output power and efficiency) versus the coupling factor or any other parameter of the external resonator will be obtained after the extraction of a bi-variate nonlinear admittance function describing the uncoupled oscillator circuit and a bi-variate DC current function, enabling the efficiency calculation. The methods have been applied to a practical power transfer system operating at 12 MHz, obtaining an experimental DC efficiency η_{DC} = 83%.

II. Oscillator Power Transfer to an External Resonator

Fig. 1 presents the cubic nonlinearity oscillator considered in the analytical formulation. At the fundamental frequency, the complex equation providing the circuit periodic solution is:

$$Y_T(V,\omega)=a+\frac{3}{4}bV^2+jC_1\omega+\frac{1}{jL_1\omega+\dfrac{jk^2L_1L_2C_2\omega^3}{1\text{-}L_2C_2\omega^2+jR_2C_2\omega}}=0 \tag{1}$$

where Y_T is the total admittance function, the nonlinear element is represented with its describing function a+3/4bV^2, having $a<0$ and $b>0$, k is the coupling factor, L_i, C_i, with i = 1, 2, are the inductor and capacitor of the first and second resonator and R_2 is the resistor in the secondary (Fig. 1). To facilitate the analysis, and considering that k is smaller than 1, we will perform a Taylor-series expansion of the second term, which will be valid up to a relatively high k. The resulting equation is:

$$\begin{aligned}Y_T(V,\omega)&\cong a+\frac{3}{4}bV^2+jC_1\omega+\frac{1}{jL_1\omega}+\frac{jk^2L_2C_2\omega}{L_1\left(1\text{-}L_2C_2\omega^2+jR_2C_2\omega\right)}\\&=a+\frac{3}{4}bV^2+jC_1\omega+Y_L(\omega)\end{aligned} \tag{2}$$

where the linear admittance $Y_L(\omega)$ shown in Fig. 1 has been introduced. The above equation can be split into real and imaginary parts:

$$Y_{T,r}(V,\omega)\cong a+\frac{3}{4}bV^2+\frac{1}{L_1}\frac{k^2L_2R_2C_2^2\omega^2}{\left(1\text{-}L_2C_2\omega^2\right)^2+\left(R_2C_2\omega\right)^2}=0 \tag{3}$$

$$Y_{T,i}(V,\omega)\cong C_1\omega\text{-}\frac{1}{L_1\omega}+\frac{1}{L_1}\frac{k^2L_2C_2\omega\left(1\text{-}L_2C_2\omega^2\right)}{\left(1\text{-}L_2C_2\omega^2\right)^2+\left(R_2C_2\omega\right)^2}=0 \tag{4}$$

As gathered from (4), the oscillation frequency varies with the coupling factor and thus with the distance between the coils.

Manuscript submitted February 20, 2021. This work was supported by the Spanish Ministry of Economy and Competitiveness and the European Regional Development Fund (ERDF/FEDER) under research project TEC2017-88242-C3-1-R.

The authors are with the Communications Engineering Department, University of Cantabria, 39005, Santander, Spain (e-mail: ardilava@unican.es, ramirezf@unican.es, suareza@unican.es;).

This article has been accepted for publication in a future issue of this journal, but has not been fully edited. Content may change prior to final publication. Citation information: DOI 10.1109/LMWC.2021.3064246, IEEE Microwave and Wireless Components Letters

If the external-resonator frequency agrees with the oscillation frequency in standalone operation, that is, $\omega_o = (L_1C_1)^{-1/2} = (L_2C_2)^{-1/2}$, the oscillation frequency will be ω_o. When analysing the circuit at the fundamental frequency only, it will keep this value for all k. Then one can simplify (3) as:

$$a + \frac{3}{4}bV^2 + \frac{1}{L_1}\frac{k^2L_2}{R_2} = 0 \tag{5}$$

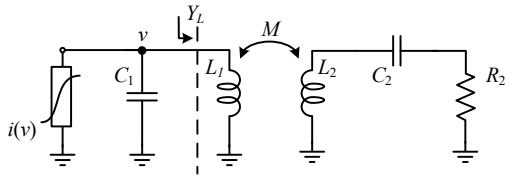

Fig. 1. Simple oscillator used in the analytical study: $C_1 = C_2 = 9.7$ pF, $L_1 = 5.6$ nH, $R_2 = 10\ \Omega$, and $i(v) = av + bv^3$ ($a = -0.01$ A/V and $b = 0.01$ A/V^3).

And the transferred power is given by:

$$\begin{aligned} P_{out} &= \frac{1}{2}\mathrm{Re}(Y_L)V^2 = -\frac{2}{3b}\frac{1}{L_1}\frac{k^2L_2}{R_2}\left(a + \frac{1}{L_1}\frac{k^2L_2}{R_2}\right) \\ &= -a\frac{2}{3b}\frac{L_2}{R_2L_1}k^2 - \frac{2}{3b}\frac{L_2^2}{L_1^2R_2^2}k^4 \end{aligned} \tag{6}$$

where Y_L is the admittance seen from the oscillator inductor when looking into the coupled resonator as shown in Fig. 1. Obviously, for $k = 0$, there is no power transfer. From a simple extreme calculation, the maximum power transfer will be obtained for the k value:

$$k_{\max}^2 = -(aR_2L_1)/(2L_2) \tag{7}$$

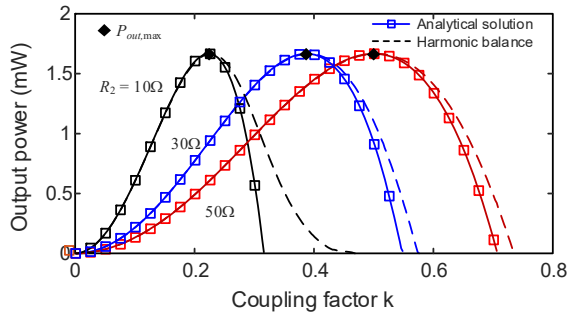

Fig. 2. Variation of the transferred power versus k for different load resistances, i.e. $R_2 = 10\ \Omega$, 30 Ω, and 50 Ω. Validation of the analytical results (solid line and square markers) with HB simulations (dashed lines).

The maximum transferred power is: $P_{out,\max} = a^2/(6b)$. Thus, under perfectly tuned conditions, the maximum transferred power depends on the oscillator only. For identical inductors, the coupling coefficient at which this maximum takes place increases with the ratio between the magnitude of the oscillator small-signal conductance $|a|$ and the conductance $1/R_2$ of the external resonator. It does not depend on the coefficient b affecting the nonlinear behaviour. From (5), a lower resistor R_2 will allow increasing the distance for the maximum power transfer. Fig. 2 presents the variation of the output power versus k, considering different values of R_2. For $R_2 = 30\ \Omega$ (blue curve), the results are overlapped with those obtained with harmonic balance (HB), at the fundamental frequency, up to $k = 0.42$. Above $k = 0.42$, the Taylor expansion in (2) becomes less accurate. As easily derived from (1), the accuracy is higher for a larger R_2, which justifies the better agreement in Fig. 2 when increasing this resistor. On the other hand, the oscillation will be extinguished in an inverse Hopf bifurcation [8] when (5) is fulfilled for $V = 0$, that is, for the k value:

$$k_H^2 = -aR_2L_1 / L_2 \tag{8}$$

Thus, in this approximate analysis, the oscillation is extinguished at $k_H = 2^{1/2}k_{\max}$. If the oscillator and external resonator frequencies are detuned, one can have more complex solutions and even disconnected solution curves under certain combinations of parameters. This is because (4) provides a cubic equation in ω^2.

III. Transistor–Based High–Power Oscillator

A. Oscillator design

The Class-E oscillator design is carried out with an original method in two stages. Initially, a Class E amplifier is obtained (Fig. 3), terminated with a coupled resonator, considering an intermediate coupling factor $k = 0.2$. For convenience, we set $R_2 = 50\ \Omega$ and calculate L_1 and C_1 for class-E operation. The two coupled inductors are equal to L_s, slightly optimized in HB to maximize the efficiency. With the transistor MOSFET IRLML0040TRPbF, excited at the frequency $f_o = 12$ MHz, a drain efficiency of $\eta_{DC} = 81\%$ was obtained ($V_{DD} = 6$V). To transform the amplifier into an oscillator, we connect an ideal box with the reflection coefficient $\Gamma = 0.999e^{j\theta}$ in series at the source terminal (Fig. 3). Then we perform a sweep in θ and, keeping the frequency constant at f_o, calculate the small-signal input admittance Y_N seen from the gate terminal (Fig. 3). The results are shown in Fig. 4. We take the θ value providing the largest negative conductance and implement it with a capacitor (for $180^o < \theta < 360^o$) or an inductance (for $0^o < \theta < 180^o$). In the case of Fig. 4a, the chosen value is $\theta = 187^o$, which at f_o corresponds to the capacitor $C_{fb} = 4$ nF. Obviously, an analogous procedure can be followed considering a parallel feedback. Next, we connect an auxiliary generator (AG) [8]–[10] at the gate terminal with the amplitude $V_{AG} = V_g$, leaving the input network in open circuit (in practice, it is loaded with a high resistor), and obtain the large-signal admittance $Y_N(V_g, \omega_o)$ as the ratio between the AG current and voltage. Then, we calculate the input network to fulfill $Y_T(V_g, \omega_o) = Y_{in}(\omega_o) + Y_N(V_g, \omega_o) = 0$, which, in this case, corresponds to an inductor in parallel with a resistor. The resistor will be useful if an injection-locked operation is desired but can be eliminated in free-running conditions. The resulting total admittance function $Y_T(V_g, \omega)$ is presented in Fig. 4b, and shows the fulfilment of the steady-state oscillation condition at V_g, ω_o. Note that the fulfilment of both the oscillation start-up condition and stability of the steady-state solution must also be verified, what has been done here with pole-zero identification [8]. The resulting oscillator output power and efficiency (without any optimization) are $P_{out} = 0.5$ W and $\eta = 83\%$.

B. Oscillator behavior versus the coupling factor

The oscillator behaviour versus the coupling factor k can be insightfully predicted extracting the oscillator nonlinear admittance function from its output terminals. This is calculated in HB with the aid of an AG, using as many harmonic terms as desired. A double sweep is carried out in ω and V, providing $Y(V,\omega)$ (Fig. 3), accounting for the whole oscillator. From the

This article has been accepted for publication in a future issue of this journal, but has not been fully edited. Content may change prior to final publication. Citation information: DOI 10.1109/LMWC.2021.3064246, IEEE Microwave and Wireless Components Letters

same double sweep, one obtains also the oscillator drain current, given by $I_{DC}(V,\omega)$. At the fundamental frequency, the oscillation condition is given by:

$$Y_T(V,\omega,k) = Y(V,\omega) - \frac{1}{jL_1\omega} + \frac{1}{jL_1\omega + \dfrac{jk^2L_1L_2C_2\omega^3}{1-L_2C_2\omega^2+jR_2C_2\omega}} = 0 \quad (9)$$

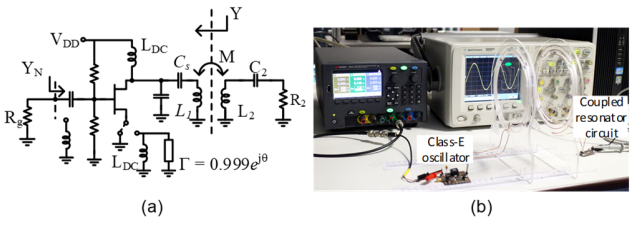

Fig. 3. Class-E oscillator. (a) Schematic with series feedback. An ideal box with $\Gamma = 0.999e^{j\theta}$ is connected in series at the source terminal. The value that maximizes the negative conductance is implemented with a reactive element. (b) Experimental setup.

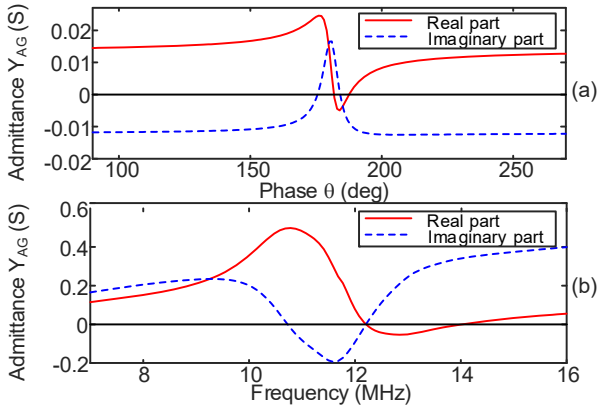

Fig. 4. Transformation of a Class–E amplifier into an oscillator. (a) Variation of the input admittance with θ. (b) Variation of the total admittance after implementing the input network to fulfill $Y_{in}(\omega_o) + Y(V_g, \omega_o) = 0$.

Note that one must subtract the inductance susceptance since oscillator admittance includes this susceptance term. Due to the filtering effects of the output network of the Class–E oscillator, (9) at the fundamental frequency will provide sufficient accuracy (HB curves are overlapped). The two functions are extracted from HB only once. Then, to obtain the variation oscillator solution versus k, one performs a sweep in k (in in-house software) and, at each k step, calculates the intersections of the contours $\mathrm{Re}\{Y_T(V,\omega,k)\} = 0$ and $\mathrm{Im}\{Y_T(V,\omega,k)\} = 0$, which will provide one or more solution points V_o, ω_o. The output power and drain efficiency are calculated interpolating the following functions at the solution points resulting from the intersection:

$$P_{out} = \frac{1}{2}\frac{k^2R_2L_1L_2C_2^2\omega^4}{(R_2C_2L_1\omega^2)^2 + \left[L_1\omega + (k^2-1)L_1L_2C_2\omega^3\right]^2}V^2 \quad (10)$$

$$\eta_{DC} = P_{out} / \left[V_{DC}I_{DC}(V,\omega)\right] \quad (11)$$

As expected, for $k = 0$, there is no power transfer. Applying this method to the oscillator in Fig. 3, for three different values of the feedback capacitor, we obtain the results shown in Fig. 5. In the three cases there is an oscillation extinction after a certain k value. Moreover, the oscillation is extinguished for a k^2 value that approaches twice the one at which the maximum power is obtained, in agreement with the theoretical derivations. The simplicity of (10) allows a simple evaluation of the oscillator behaviour under any change in the parameters of the coupling network. The condition for the oscillation extinction is:

$$\begin{aligned} Y_r(0,\omega) + \frac{k^2R_2L_1L_2C_2^2\omega^4}{(R_2C_2L_1\omega^2)^2 + \left[L_1\omega + (k^2-1)L_1L_2C_2\omega^3\right]^2} &= 0 \\ Y_i(0,\omega) - \frac{(R_2C_2)^2L_1\omega^3 + \left[L_1\omega + (k^2-1)L_1L_2C_2\omega^3\right](1-L_2C_2\omega^2)}{(R_2C_2L\omega^2)^2 + \left[L_1\omega + (k^2-1)L_1L_2C_2\omega^3\right]^2} &= 0 \end{aligned} \quad (12)$$

where $Y(0,\omega)$ indicates the oscillator admittance in small-signal conditions. Sweeping R_2 and solving for k and ω one obtains the locus for the oscillation extinction.

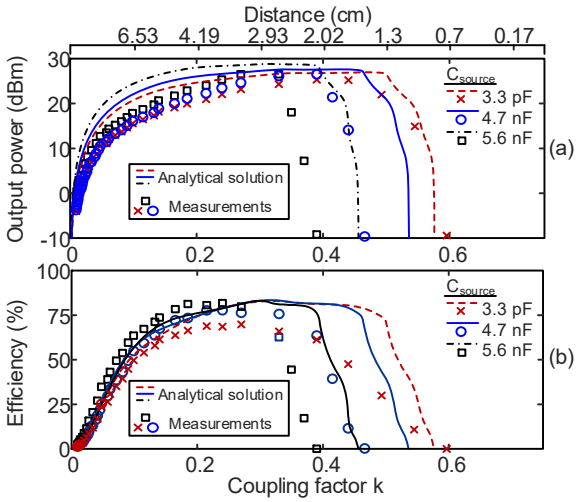

Fig. 5. Variation of the oscillator (a) output power and (b) efficiency versus k for three different values of the feedback capacitor. HB results are overlapped. The distance between the inductors is indicated in the upper axis.

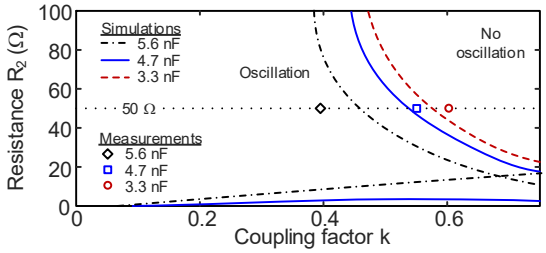

Fig. 6. Locus for the oscillation extinction in the plane defined by k and R_2. Three different values of the feedback capacitor have been considered. Experimental results for the load resistor $R_2 = 50\ \Omega$ are superimposed.

IV. Conclusion

An in-depth investigation of the power transfer of an oscillator to an external resonator has been presented. An analytical study demonstrates the extinction of the oscillation from certain value of the coupling factor. A simple feedback method to obtain a high-power oscillator from a Class-E amplifier has been provided. The oscillator solution curves versus the coupling factor and the elements of the external resonator are obtained with a bi-variate nonlinear admittance function accounting for the oscillator circuit, combined with the passive admittance of the coupled resonator. Very good results have been obtained in comparison with the measurement results.

REFERENCES

[1] A. Jarndal, T. Petrovic, "GaN-Based Oscillators for Wireless Power Transfer Applications," *Int. Conf. Advanced Computation and Telecommunication*, Bhopal, India, 2018, pp. 1-5.

[2] D. Rattanarungngam, K. Phaebua, T. Lertwiriyaprapa, "Power control unit for E-class power oscillator of 6.78 MHz wireless power transfer," *Int. Symp. Ant. Prop.*, Phuket, 2017, pp. 1-2.

[3] R. L. O. Pinto, R. M. Duarte, F. R. Sousa, I. Mïller, Brusamarello, V., "Efficiency modeling of class-E power oscillators for wireless energy transfer," *IEEE Int. Inst. Meas. Techn. Conf.*, Minneapolis, MN, 2013, pp. 271-275.

[4] Y. Yamashita, K. Wada, "Wireless power transmitter using parallel-tuned class-E power oscillator," *Int. Symp. Elect. Smart Dev.*, Yogyakarta, 2017, pp. 287-290.

[5] R. Chai, A. Mortazawi, "A Coupling Factor Independent Wireless Power Transfer System Employing Two Nonlinear Circuits," *IEEE MTT-S Int. Microw. Symp. (IMS)*, Los Angeles, CA, USA, 2020, pp. 393-396

[6] A. Suárez, R. Melville, F. Ramírez, "Analysis and Synthesis of Hysteresis Loops in an Oscillator Frequency Characteristic," IEEE Trans. Microw. Theory Techn., vol. 67, no. 12, pp. 4890-4904, Dec., 2019.

[7] A. Suárez, R. Melville, F. Ramírez, "Coupling-induced hysteresis in free-running oscillators," *IEEE MTT-S Int. Microw. Symp. (IMS)*, Boston, MA, USA, Jun., 2019.

[8] A. Suárez, S. Sancho, F. Ramírez. "General Formulation for the Analysis of Injection–Locked Coupled–Oscillator Systems," *IEEE Trans. Microw. Theory Techn.*, vol. 61, no. 12, pp. 4730–4744, Dec., 2013.

[9] M. Pontón, E. Fernández, A. Suárez, F. Ramírez, "Optimized design of pulsed waveform oscillators and frequency dividers," *IEEE Trans. Microw. Theory Techn.*, vol. 59, no. 12, pp. 3428–3440 , Dec., 2011.

[10] F. Ramírez, S. Sancho, A. Suárez, "Oscillation modes in multiresonant oscillator circuits," *IEEE Trans. Microw. Theory Techn*., vol. 64, no. 12, pp. 4660-4675, Dec., 2016.